Cryst. Res. Technol. **42**, No. 9, 867 – 875 (2007) / **DOI** 10.1002/crat.200710918

Spray pyrolysis deposition and characterization of highly (100) oriented magnesium oxide thin films

A. Moses Ezhil Raj[1], L. C. Nehru[2], M. Jayachandran[2], and C. Sanjeeviraja*[3]

[1] Department of Physics, Scott Christian College, Nagercoil-629003, India
[2] ECMS Division, Central Electrochemical Research Institute, Karaikudi-630006, India
[3] Department of Physics, Alagappa University, Karaikudi-630003, India

Received 6 January 2007, revised 3 May 2007, accepted 12 May 2007
Published online 20 June 2007

Key words thin films, dielectric, magnesium oxide.
PACS 77.55.+f

Transparent dielectric thin films of MgO has been deposited on quartz substrates at different temperatures between 400 and 600°C by a pneumatic spray pyrolysis technique using $Mg(CH_3COO)_2.4H_2O$ as a single molecular precursor. The thermal behavior of the precursor magnesium acetate is described in the results of thermogravimetry analysis (TGA) and differential thermal analysis (DTA). The prepared films are reproducible, adherent to the substrate, pinhole free and uniform. Amongst the different spray process parameters, the substrate temperature effect has been optimized for obtaining single crystalline and transparent MgO thin films. The films crystallize in a cubic structure and X-ray diffraction measurements have shown that the polycrystalline MgO films prepared at 500°C with (100) and (110) orientations are changed to (100) preferred orientation at 600°C. The MgO phase formation was also confirmed with the recorded Fourier Transform Infrared (FTIR) results. The films deposited at 600°C exhibited highest optical transmittivity (>80%) and the direct band gap energy was found to vary from 4.50 to 5.25 eV with a rise in substrate temperature from 500 to 600°C. The measured sheet resistance and the resistivity of the film prepared at 600°C were respectively $10^{13}\Omega/\square$ and $2.06 \times 10^{7}\Omega$ cm. The surface morphology of the prepared MgO thin films was examined by atomic force microscopy.

1 Introduction

MgO is a highly ionic crystalline solid, which crystallizes into a rock salt structure. It has fcc Mg^+ and O^- sub-lattices, and low energy neutral (100) cleavage planes. The lattice constant of MgO is 0.421 nm and its refractive index and dielectric constant are 1.736 and 10 respectively. Magnesium oxide seems to be a good candidate regarding its bulk properties: large band gap (7.8 eV), high thermal conductivity and stability and an alternative dielectric to silicon dioxide (SiO_2) to reduce the electric field in capacitive networks [1]. MgO, widely used as a substrate for high-temperature superconductor films deposition, has attracted much attention due to its low dielectric constant, low dielectric loss, and less mismatch with YBCO films [2]. With a low dielectric loss, MgO shows a wide application in microwave devices. Due to its low refractive index, MgO is especially a suitable buffer for epitaxial optical waveguide films [3]. Ceramic or metal/alloy oxide films are of scientific and technological importance due to their applications in optical and electronic devices, in catalytic reactions, as protective coatings on metals, as single tunnel barriers and in gas sensors. They are mostly preferred due to their wide band gap and inertness against many chemical reactions [4]. Interestingly, ceramic oxide thin film substrates are used as support for different metallic films or multi-layers. These applications need the growth of epitaxial insulating films with single crystalline nature and surface smoothness of few nanometer levels. Fundamentally also, MgO with its simple cubic rock salt structure is an attractive model system to investigate oxide surface chemistry. Since it is a prototypical ionic insulator with a wide band gap,

* Corresponding author: e-mail: sanjeeviraja@rediffmail.com

motivation is high to grow MgO films on a conductive substrate useful for charged-particle measurement, in addition to the applications mentioned above. Moreover, the usefulness of MgO films as buffer layers for the growth of high T_c superconducting [5], and ferroelectric [6,7] films has led to an increased interest in the growth of this material. The most important point in these applications is the preparations of highly (100) oriented MgO thin films that can prevent inter-diffusion between the superconducting films and substrate and solve chemical reactivity at higher temperatures [8]. In thin film devices developments, the structural and morphology of the film-substrate interface can greatly alter the resulting film properties [9]. Unlike the situation with metals and semiconductors, ionic oxide surfaces are more complex, and high quality crystalline oxide surfaces are difficult to prepare. If a device-quality epitaxial MgO buffer films could be grown on any substrate like metal/semiconductor/insulator, it will be considered a monocrystalline quality surface with few defects.

MgO films can be prepared by a variety of deposition techniques including laser ablation [10,11], electron beam evaporation [12,13], metal organic chemical vapor deposition [14], magnetron sputtering [15,16], ion beam assisted deposition [17] and spray pyrolysis [18,19]. The spray pyrolysis is one of the simplest deposition techniques because of its simplicity and provides large area coatings without high vacuum ambience. So the capital cost and the production cost of high quality metal oxide thin films are expected to be the lowest among all the thin film deposition techniques. Furthermore, this technique is also compatible with mass production system. Also, the coatings produced with the spray pyrolysis are inherently uniform and the surface to volume ratio of the nanodrops are very large making them very receptive to heat treatment and pyrolysis. Further, relatively moderate temperature heat treatment is only necessary for the growth of highly oriented thin films on different semiconductor substrates for device developments.

Recently, Rhee et al. [20] deposited (100) oriented MgO thin films on Si (111) and amorphous glass substrates using the charged liquid cluster beam technique in air using magnesium acetate precursor in ethanol with an acid catalyst. Similar preferential growth morphology on different substrates like Si (100) [21], alumina coated sapphire [22] and corning 7059 glass [23] using various precursors (Mg 2,4-pentanedionate, bis 2,2,6,6-tetramethyl-3,5-heptanedionato magnesium) in different solvents have been reported by many research groups. In this paper, we report the preliminary results on the growth of MgO thin films on quartz substrates using hydrated magnesium acetate [Mg $(CH_3COO)_2.4H_2O$] as precursor in ethanol with tri-ethylene glycol (TEG) suitable for high temperature processing. The deposition conditions employed in this study enabled us to deposit thin films of MgO on quartz substrates without cracking and inter-diffusion. The structural, optical, electrical and morphological properties are reported.

2 Experimental

Chemical spray pyrolysis is one of the major techniques used to deposit a wide variety of materials including metal/alloy oxides. The experimental work of spray pyrolysis for growth of MgO thin film was carried out in a reaction chamber, schematically illustrated in figure 1. The deposition system consists of four sections which includes: (a) the reactants and carrier gas assembly connected to the spray nozzle at the entrance of the reaction chamber, (b) the reaction chamber in which there is a resistive heater used to heat the substrate to the required temperature for thin film deposition, (c) the temperature controller that monitors the deposition temperature and controls the desired substrate temperature and (d) the exhausting gas module. The substrate temperature was measured using a chromel-alumel thermocouple to an accuracy of ± 1 K.

In the present work, thin films of MgO were prepared on quartz substrates using metal-organic magnesium acetate precursor. The spray solution was prepared by dissolving different amounts of magnesium acetate for predefined molarity in the solvent containing 90% ethanol, 5% HCl and 5% TEG. Ethanol has a very low boiling point (~ 80°C) and therefore, high substrate temperature causes the spray solution cone to partially evaporate even before they hit the substrate. This makes the surface morphology of the deposited films highly uneven and powdery. In order to prevent these undesired morphologies, TEG is added, which has a high boiling point (~ 280°C). Addition of TEG reduces both premature evaporation of the solvent in the spray cone while in transit from the spray nozzle to the substrate and the resultant loss of material during the condensation due to the high substrate temperature. The spraying solution is always buffered by a small amount of hydrochloric acid to increase the solubility and prevent precipitation in the solution.

The substrates were well cleaned, just prior to deposition with hot chromic acid, followed by rinsing with acetone, methanol, and isopropanol and finally cleaned ultrasonically in deionized water. Then the starting

solution was sprayed onto the hot substrate kept at a distance of 30 cm below the spray gun nozzle using air as carrier gas. The preparative parameters of the system viz. solution spray rate, precursor concentration, volume of sprayed solution and carrier gas pressure were optimized to obtain uniform, pinhole free and adherent films after conducting many trails. The substrate temperature was varied from 400 to 600°C. The prime requisites for obtaining good quality MgO thin films are the optimization of above-mentioned preparative conditions and are given in table 1.

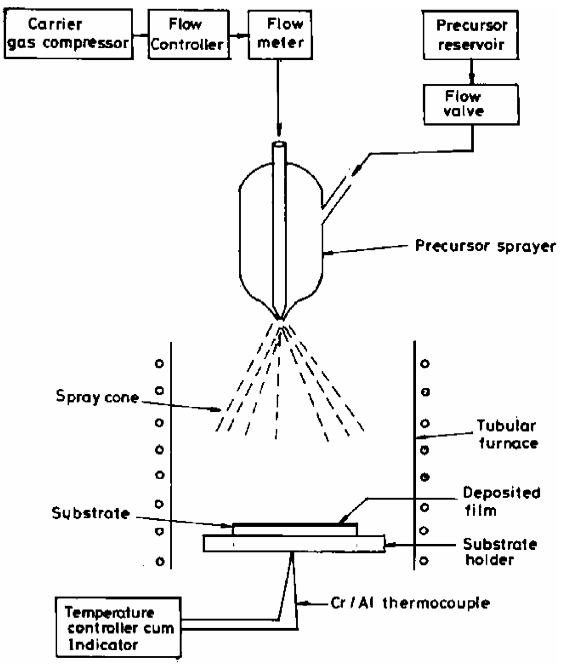

Fig. 1 Experimental spray pyrolysis set-up.

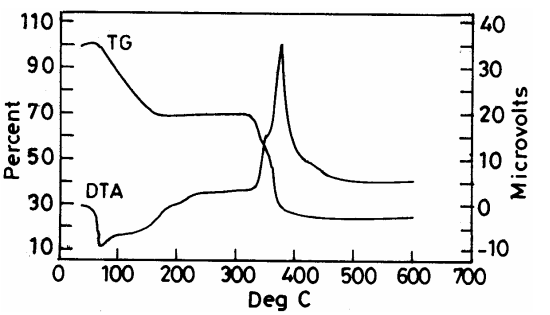

Fig. 2 TGA/DTA thermograms of the starting precursor magnesium acetate.

Table 1 Optimized deposition conditions for the preparation of MgO thin films

Spray parameters	Values
Concentration of precursor	0.15 M
Volume of precursor sprayed	50 ml
Solvent	90% Ethanol + 10% TEG
Substrate temperature	400-600°C
Spray rate	5 ml/min
Carrier gas pressure	0.4 kg/cm^2
Nozzle-substrate temperature	30 cm

Thermogravimetry analysis (TGA) and differential thermal analysis (DTA) of the magnesium acetate ($Mg(CH_3COO)_2.4H_2O$, AR grade purity 99.9%) was carried out using TA instrument (simultaneous TGA-DSC). The film thickness was measured with the aid of a surface profiler and also using weight difference method, considering the density of bulk magnesium oxide (3.563 g/cm^3). The thicknesses of the deposited films were in the range between 0.3 and 0.6 μm. The structural properties of the deposited films were studied by x-ray diffraction measurements using CuK_α radiation with λ = 1.5404 Å. The average crystallite size and the related structural properties of the MgO film were estimated from the classical Scherrer's and other formulae [24]. The FTIR spectra of the films were recorded using Perkin-Elmer FTIR spectrophotometer in the spectral range 400-4000 cm^{-1}. The optical absorption measurements in the range 200-1500 nm were carried out in a 'Hitachi 330' spectrophotometer at room temperature. High precision electrometers were used to measure the current and voltages; where as the temperature of the specimen was measured with a digital thermometer to a precision of 0.01 K. The surface morphology of the films was investigated by atomic force microscopy (Nanoscope).

3 Results and discussion

MgO formation and film growth mechanism The thermal decomposition behavior of Mg $(CH_3COO)_2$. $4H_2O$ precursor was studied using TGA and DTA. The TGA and DTA were performed in the temperature range 30-700°C with alumina as reference material at a scan rate of 10 K/min. The DTA chamber was purged with air at a flow rate of 75 cm^3/min.

The TGA curve of hydrated magnesium acetate precursor (Fig. 2) is essentially a three steps process in which the inflection point coincides with the temperature corresponding to minima and maxima in DTA trace. The thermal decomposition reaction follows the stoichiometry [25]:

$$Mg(CH_3COO)_2.\ 4H_2O \rightarrow Mg(CH_3COO)_2 + 4H_2O$$

$$Mg(CH_3COO)_2 \rightarrow MgCO_3 + (CH_3)_2.CO\ (g)$$

$$MgCO_3 \rightarrow MgO + CO_2\ (g)$$

The weight loss of precursor begins as heating is applied at 50°C. The first mass loss occurs over the temperature range 61 - 168°C; the mass loss of 31.64% is slightly less than the loss of 4 moles of water per mole of salt (33.60%). This mass loss corresponds to removal of physisorbed molecules of water. The second stage starts at about 168°C, which is due to the onset of decomposition of the dehydrated $Mg(CH_3COO)_2$ that proceeds slowly until 346°C. The reaction is completed with a mass loss of 27.09% for the release of acetone in gaseous phase. The calculation of residue between these temperature ranges clearly indicates the formation of intermediate $MgCO_3$ phase. At the third step, the reaction becomes extremely rapid, leading to a final loss of 20.52%. This value is nearly the same as that predicted for the formation of metallic magnesium oxide by exhausting CO_2. At about 500°C, MgO phase was formed which remains stable up to 600°C. The final residue MgO should have a mass percentage of 18.7, which is confirmed from the TGA analysis. Beyond 500°C no further weight loss takes place up to 600°C, indicating formation of stoichiometric MgO. Therefore, it is anticipated that the films deposited at various substrate temperature below 500°C were of amorphous, since the crystallization process is incomplete until 500°C.

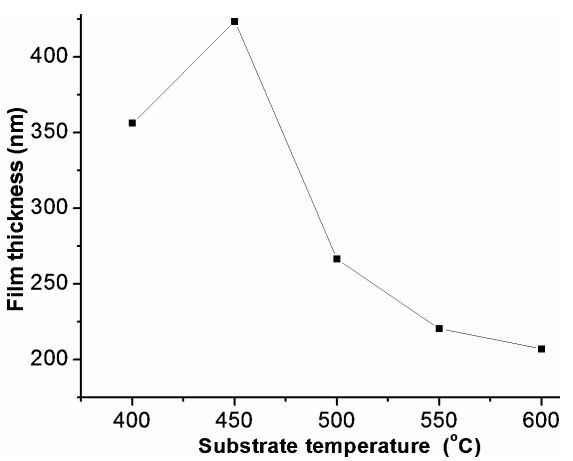

Fig. 3 Growth rate variation in terms of substrate temperature.

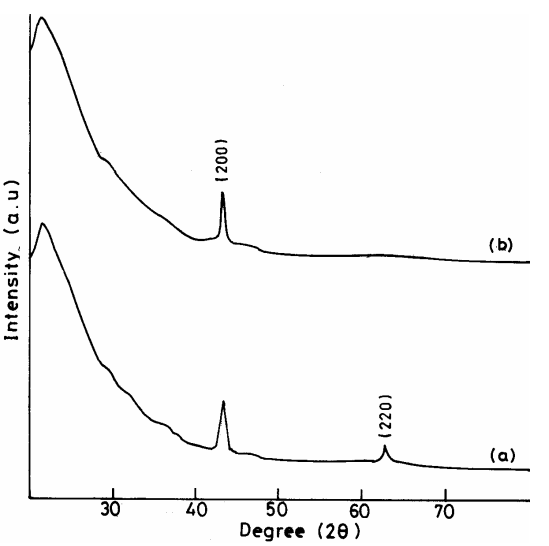

Fig. 4 X-ray spectra of MgO films deposited at (a) 500°C (b) 600°C.

After analyzing various stages associated with the decomposition of the starting precursor (Mg salt), it is concluded that the films prepared below the substrate temperature 400°C are of mixed amorphous and polycrystalline nature and those prepared above 500°C are fully crystallized with preferred orientations.

The growth of MgO film in relation to the substrate temperature is investigated. At low temperatures, the growth rate is controlled by activated processes such as adsorption, surface diffusion, chemical reaction and desorption. The growth rate is thus controlled by the reaction kinetics. This means that the molecules, which are flowing by diffusion, accumulate in front of the substrate and hence the concentration gradient flattens. But

at higher temperatures all molecules that are diffusing towards the substrate will be deposited. These activated processes occur so fast that the molecules flowing to the substrate do not damp up. The concentration gradient remains steep, i.e. the growth rate is diffusion limited. The dependence of the MgO film growth on substrate temperature, by varying the temperature between 400-600°C, is shown in figure 3. The growth rate is 35, 26, and 20 nm/min. for the films deposited at 400, 500 and 600°C respectively. It can be seen that the deposition rate decreases with the increase of substrate temperature, despite the fact that the kinetics of MgO forming reaction increase with increasing temperature. This dependence can be explained on the basis of the reactions associated with the low-temperature chemical deposition processes [26]. The diminished mass transport to the substrate at higher temperature may be due to gas convection from the substrate pushing back the droplet vapors of the precursor away from the substrate. Further, the sticking coefficient of Mg is reduced at high temperatures [27]. Additionally, the decrease of film deposition rate is also related to the increase of film density with increasing temperature. The higher diffusion energy supplied by the higher temperature is to fill in the internal defects, which results in the formation of denser films [28,29]. So, MgO films deposited at 600°C have higher density values, which could restrict the inter-diffusion of Mg atoms and H_2O thereby providing an increased chemical stability under various working conditions [30].

Structural properties As seen from the TG/DTA observations, stoichiometric MgO crystallization starts only for substrate temperatures above 400°C and the films deposited below this temperature showed only amorphous nature. Figure 4 shows the typical x-ray spectra of MgO films prepared at 500 and 600°C. As seen from the spectra, the films are crystalline in nature with a cubic fcc-cp structure according to the JCPDS standards (PDF # 89 -7746).

It is observed that the films deposited at 500°C are polycrystalline with two peaks at $2\theta = 43.12°$ and 62.47° and they correspond to the (200) and (220) reflections of MgO indicating the presence of randomly oriented crystallites. No characteristic peaks of impurity and other phases have been observed. Comparatively, the intensity of (200) plane becomes progressively more dominant. With increase of substrate temperature to 600°C, the films are strongly textured with preferential orientation along the (200) axis representing the formation of single crystal films with cubic structure. Whereas the intensity of (220) peak shows a decreasing trend and disappears completely. Moreover, with increase in temperature, the Full Width at Half Maximum (FWHM) of (200) plane becomes narrower which indicates the improvement in the structural order of MgO films. The increase of intensity of (200) peak can be attributed to the improvement in the crystallinity at higher temperature and facilitating reorientation of all the crystallites along (100) direction. This improvement in the structural order can also be attributed to the increase in the film density [31].

The observed relationship between the degree of (200) preferred orientation and the deposition temperature may be explained in terms of the migration of molecules onto the growing surface. MgO is expected to achieve a (200) preferential orientation that has a lower energy configuration during nucleation. The number of absorbed Mg and O atoms with higher mobility are enhanced at higher substrate temperature that could easily move to equilibrium atomic sites on the surface i.e. the (200) plane of MgO which is energetically stable [32]. Thus the domination of (200) preferential orientation occurs when the substrate temperature is optimum enough to arrange the atoms with minimum defects and with maximum packing density. Also, it is expected that the thermal energy of the substrate provides the migration energy for the surface atoms to form stable (200) preferential layer.

The crystallite size 'D' of MgO was calculated for the (200) and (220) diffraction peaks using the Scherrer's formula [33]:

$$D = \frac{K\lambda}{\cos\theta\sqrt{\beta^2 - \beta_0^2}}$$

where, K=0.94, λ is the wavelength of incident x-ray radiation (1.5404 Å for CuK_α), β is the intrinsic full width at half maximum of the peak, β_0 is the integral peak width caused by instrumental broadening and θ is the Bragg's diffraction angle of the respective XRD peak. Using this data, the dislocation density (δ) can be calculated from $\delta = 1/D^2$, the micro strain (ε) can be calculated from $\varepsilon = (\lambda/D\sin\theta)-(\beta/\tan\theta)$ and the number of crystallites/ unit area (N) is found out from $N = t/D^3$ which will elucidate the nature of the prepared MgO films. The measured line-widths and the other above mentioned values are calculated and are given in table 2.

Table 2 Observed lattice parameters as a function of temperature for MgO thin films prepared by spray pyrolysis.

Substrate Temperature (°C)	Reflecting plane (hkl)	d spacing (Å) observed	d spacing (Å) JCPDS Standards	Lattice constant (Å) Observed	Lattice constant (Å) Standard	Crystallite size, D (nm)	Dislocation density, δ 10^{11} lines/cm^2	Strain, ε 10^{-3}	Number of crystallites 10^{10}/cm^3
500	(200)		2.1099	4.2198	4.219	30.12	1.10	1.16	0.9732
	(220)	1.4968	1.4919	4.2335		16.04	3.86	1.118	6.43
600	(200)	2.1084	2.1099	4.2168	4.219	34.12	0.879	0.75	0.206

At 500°C, the film has mainly two categories of crystallites of larger (200) oriented crystallites with 30.1 nm grain size and smaller (220) oriented crystallites with 16.04 nm size. At 600°C, the crystallinity increases with (200) preferred orientation only with a grain size of 34.12 nm. The reason for (200) preferred orientation is that the number of oxygen vacancies is higher due to the reduced sticking coefficient of oxygen at high temperatures [36]. This is due to the fact that smaller grains with (220) orientations tend to have surfaces with sharper convexity; they gradually disappear by feeding the larger grains, as temperature increases. Also, this size increase of the (200) oriented crystallites at 600°C reveals partial annealing of the film at higher temperature, which provided restructuring of the film making it to be of monocrystalline nature. Formation of (200) oriented MgO films is advantageous that MgO (100) is a superb substrate for the epitaxial growth of Fe_2O_4 and γFe_2O_3 from a crystallographic point of view [37].

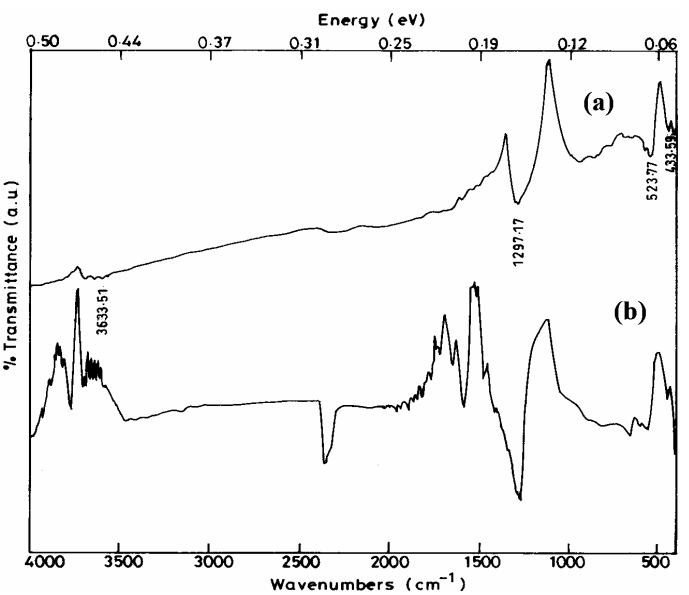

Fig. 5 FTIR spectrum of MgO film deposited at (a) 600°C, (b) 500°C.

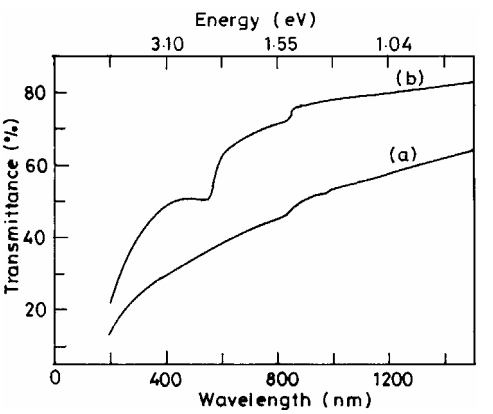

Fig. 6 Transmittance spectra of MgO processed at (a) 500°C (b) 600°C.

FTIR spectroscopy The FTIR spectroscopic results give information about phase composition and the way in which oxygen is bound to metal ions. Figure 5(a) shows the FTIR spectrum of the MgO film deposited at 600°C, which indicates the complete thermal conversion of the precursor into oxide. The spectrum comprises five transmission bands at 407 cm^{-1}(ν_1), 533 cm^{-1}(ν_2), 966 cm^{-1}(ν_3), 1228 cm^{-1}(ν_4) and 3634 cm^{-1}(ν_5). The very small peak observed at 3634 cm^{-1} can be assigned to hydrogen-bonded hydroxyl groups and $Mg(OH)_2$ [38]. The broad peaks at 1228 cm^{-1} and 966 cm^{-1}could be assigned to the deformation band in water and to the C-O stretching absorption in the bicarbonate and carbonate ions [39]. These impurities most likely originate from the precursor and solvent or from exposure to the atmosphere. It is well known that H_2O and CO_2 molecules are chemisorbed on to randomly oriented MgO surfaces when exposed to the atmosphere. Therefore, a small amount of impurity is likely to be incorporated in the film during its exposure to ambient atmosphere. The Mg-O absorption peaks are expected in the 400-600cm^{-1} region. The sharp peaks seen at 533 and 482 cm^{-1} are associated with the longitudinal optical (LO) phonon modes of MgO lattice. This implies that the film consists mostly of MgO with a small concentration of hydroxide and carbonate impurities. The wave number of Mg-O desorption in pure ionic magnesium oxide is ~ 425 cm^{-1} [40]. MgO film prepared at 500°C,

exhibits additional intense peaks in the FTIR spectrum (Fig. 5b) and these peaks could be due to adsorption of more water on exposing the films to the atmosphere. As these films are less dense, they are easily prone to hydration by forming $Mg(OH)_2$.

Optical absorption studies The optical absorption spectra for the as-deposited films were recorded in the wavelength range 200-1500 nm. Figure 6 shows the optical transmittance curve as a function of the wavelength for the MgO films deposited at various substrate temperatures. The absorption co-efficient of the films were found to be of the order of 10^4 cm^{-1}. The percentage of transmission (%T) value in the visible region is found to increase with increase in substrate temperature. Maximum transmission behavior is observed for the MgO films prepared at 600°C and comparatively lower transmission values are recorded for the films prepared at 500°C. The increase in %T is attributed to the well adherent and crystalline nature of the film throughout the coated area, which is obtained due to uniform oxidation and improvement in lattice arrangements, resulting in better optical properties.

In order to confirm the nature of optical transition in these samples, the optical data were analyzed using the classical equation

$$\alpha = \alpha_o \frac{(h\nu - E_g)^n}{h\nu}$$

where, 'E_g' is the separation between the bottom of the conduction band and the top of the valence band, '$h\nu$' the photon energy and 'n' is a constant.

For allowed direct transition n = 1/2 and for allowed indirect transition n = 2. The plots of $(\alpha h\nu)^2$ against $h\nu$ for all the as deposited samples are shown in figure 7. The nature of plot suggests direct inter-band transition. The extrapolation of straight-line portion to zero absorption co-efficient ($\alpha = 0$) leads to the estimation of band gap energy. The band gap energy (E_g) of samples deposited at 600°C is 5.25 eV, whereas the films processed at 500°C is 4.5 eV. Generally, it can be stated that this reduced band gap energy of MgO may be due to varied extent of non-stoichiometry of the deposited layers. But, interestingly these observed band gap energies of MgO films are invariably lower than the band gap value of bulk MgO (7.8 eV) which may be due to the various lattice associated atomic interaction phenomena come into play from its ionic crystalline nature [41].

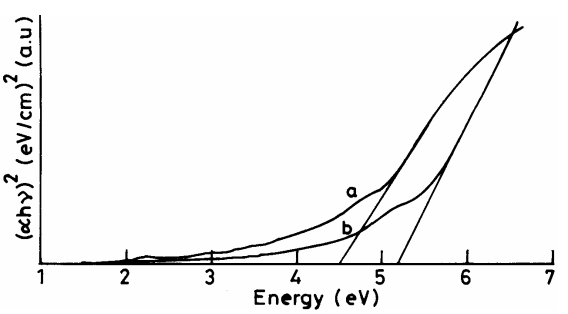

Fig. 7 Band gap variation as a function of substrate temperature: (a) 500°C, (b) 600°C.

As far as ionic crystal lattice is concerned, the band gap separation or variation is entirely different in thin films compared to bulk material [42]. Here the energy gap between the conduction band and the valence band is perturbed which is mainly depends on the following electronic structure characteristics [43]: (i) the Madelung energy due to charge-charge interactions in the system, (ii) the delocalization energy due to electron sharing between atoms, (iii) the internal energy due to the filling of atomic orbital and intra-atomic electron-electron interactions and (iv) the short-range repulsion energy between atoms that makes the atoms not to come close to each other. In addition, the presence of oxygen vacancies also induce changes in the electronic structure of surfaces. On planner surfaces, the Madelung potential is weakened leading to a reduction of the ionic gap and in turn its total band gap becomes smaller compared to bulk. On the rock salt plane (100) and faceted (110) surfaces, the ratios of surface to bulk Madelung potential are 0.96 and 0.88 respectively. Further, 1% and 5% bond contractions are found on (100) and (110) faces, on which the surface atoms have 5 and 4 first neighbors. Also, the electron redistribution takes place on the magnesium atoms, which are located close to the oxygen vacancies. Their effective atomic levels are shifted towards low energies (3s levels) or high energies (3p levels), indicating a splitting of the conduction band and the presence of a gap state. The Fermi level is pinned on this gap state, which is partly filled except when all oxygen have left the surface [44].

Electrical properties The electrical transport properties of MgO films strongly depend on their structure (grain size and shape, defects etc), purity (concentration of impurities like absorbed and adsorbed gases, moisture, etc) and on the preparation conditions. The resistivities of the films were directly measured by the two-probe technique. A known potential was applied across the end contacts of the sample and the current was measured with a high precision electrometer. At room temperature, the sheet resistance of MgO films prepared at 600°C was of the order of $10^{13}\Omega/\square$, where as for the films prepared at 500°C had less resistance of $7.98\text{x}10^{12}\Omega/\square$. The respective resistivity values are $2.06\text{x}10^{7}\Omega$ cm and $2.12\text{x}10^{6}\Omega$ cm and these values are in agreement with the results reported by DeSisto and Henry [45] for the spray deposited MgO films from the precursor Mg(2,4-pentanedionate)$_2$.

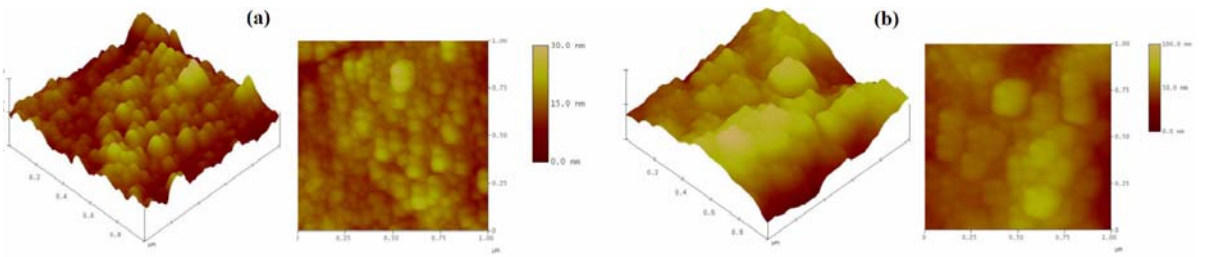

Fig. 8 AFM micrograph of MgO film deposited at (a) 500°C, (b) 600°C.

Surface morphology AFM resolved nano-sized particulate microstructure of the MgO film deposited at 600°C is shown in figure 8. As seen, the surface topography of the deposited film is smooth and homogeneous. The observed whole area of the specimen had a relatively continuous and flat surface with some isolated MgO islands. The formation of these MgO islands is considered to result from high-speed migration of deposited species in the case of the high temperature growth and a relatively large interfacial free energy between the substrate and the film. From AFM images, root mean square (RMS) surface roughness value was measured to indicate the film surface roughness quantitatively. RMS value of the film deposited at 600°C is about 18 nm, which indicates that the surface of the spray deposited MgO thin film is very smooth. In order to study the surface morphology, line profile analysis was performed and result indicated that the MgO surface was considerably flat and parallel to the substrate. Further, the grain size of the film can also be deduced from the AFM micrograph and the distribution of grain size value is observed between a minimum of about 50 nm and a maximum of about 125 nm. The statistical mean grain size of the film deposited at 600°C is about 71nm, which is about two and a half times the crystallite size calculated from the XRD profile.

4 Conclusion

Magnesium oxide films have been successfully prepared on quartz substrates at temperatures 500 and 600°C using the spray pyrolysis technique. The process parameters were optimized to have good quality crystalline films. The films were optically clear, adherent and uniform. Growth rate and crystalline quality were sensitive to the substrate temperature. MgO film started to crystallize above 400°C and preferentially oriented in the (200) direction as the substrate temperature increased to 600°C. At 500°C, preferential peak along (220) orientation was also detected. The Mg-O phase formation was identified from the FTIR results. All the films were transparent in the visible and IR range of radiation, with transparency greater than 80% and the associated band gap value is 5.25 eV when the substrate temperature is increased to 600°C. The resistivity of the films prepared was in the order of $10^{7}\Omega$ cm. AFM studies confirmed the uniformity and well grown crystalline morphology of the MgO films prepared at the optimum temperature.

References

[1] K. Nashimoto, D. K. Fork, and T. H. Geballe, Appl. Phys. Lett. **60**, 1199 (1992).
[2] F. Ahmed, K. Sakai, H. Ota, R. Aokl, N. Ikemiya, and S. Hara, J. Low Temp. Phys. **105**, 1343 (1996).
[3] X. L. Guo, Z. G. Lu, X. Y. Chen, S. N. Zhu, S. B. Xiong, W. S. Hu, and C. Y. Lin, J. Appl. Phys. **29**, 1632 (1996).
[4] V. E. Henrich and P. A. Cox, "The Surface Science of Metal Oxides", Cambridge Univ. Press, Cambridge (1994).

[5] A. B. Berezin, C. W. Yuan, and A. L. de Lozanne, Appl. Phys. Lett. **57**, 90 (1990).
[6] L. D. Chang, M. Z. Tseng, E. L. Hu, and D. K. Fork, Appl. Phys. Lett. **60**, 3129 (1992).
[7] S. Fujii, A. Tomozawa, E. Fujii, H. Torri, R. Takayamma, and T. Hirao, Appl. Phys. Lett. **65**, 1463 (1994).
[8] L. A. Lipkin and J. W. Palmour, IEE Trans Electron Dev. **46**, 546 (1999).
[9] T. Yoshimura and N. Fuji Mura, J. Cryst. Growth. **174**, 790 (1997).
[10] P. A. Stample and R. J. Kennedy, Thin Solid Films **326**, 63 (1998).
[11] E. J. Tarsa, X. H. Wu, J. B. Ibbertson, J. S. Speck, and J. J. Zinck, Appl. Phys. Lett. **66**, 3588 (1995).
[12] L. S. Huang, L. R. Zheng, and T. N. Blanton, Appl. Phys. Lett. **60**, 3129 (1992).
[13] A. Masuda and K. Nashimoto, Jpn. J. Appl. Phys. **33**, L793 (1994).
[14] J. H. Boo, S. B. Lee, K. S. Yu, W. Koh, and Y. Kim, Thin Solid Films **341**, 63 (1999).
[15] C. H. Park, W. G. Lee, D. H. Kim, H. J. Ha, and J. Y. Ryu, Surf. Coat. Technol. **110**, 128 (1998).
[16] W. Y. Hsu and R. Raj, Appl. Phys. Lett. **60**, 3105 (1992).
[17] L. Dong, L. A. Zepeda-Ruiz, and D. J. Srolovitz, J. Appl. Phys. **89**, 4105 (2001).
[18] S. G. Kim, J. Y. Kim, and H. J. Kim, Thin Solid Films **376**, 110 (2000).
[19] J. M. Bian, X. M. Li, T. L. Chen, X. D. Gao, and W. D. Yu, Appl. Surf. Sci. **228**, 297 (2004).
[20] S. H. Rhee, Y. Yang, H. S. Choi, J. M. Myoung, and K. Kim, Thin Solid Films **396**, 23 (2001).
[21] X. Fu, G. Wu, S. Song, Z. Song, X. Duo, and C. Lin, Appl. Surf. Sci. **148**, 223 (1999).
[22] W. J. DeSisto and R. L. Henry, Appl. Phys. Lett. **56**, 2522 (1990).
[23] S. G. Kim, K. H. Choi, J. H. Eun, H. J. Kim, and C. S. Hwang, Thin Solid Films **377-378**, 694 (2000).
[24] H. P. Klung and L. E. Alexander, "X-ray Diffraction Procedures for Polycrystalline Amorphous Material", Wiley, New York (1974).
[25] M. D. Judd, B. A. Plunkett, and M. I. Pope, J. Thermal. Anal. **6**, 555 (1974).
[26] J. C. Viquie and J. Spitz, J. Electrochem. Soc. **122**, 585 (1975).
[27] S. M. Lee, H. Murakami, and T. Ito, Appl. Surf. Sci. **175-176**, 517 (2001).
[28] M. Krunks and E. Mellikov, Thin Solid Films **270**, 33 (1995).
[29] X. Fu, G. Wu, and S. Song, Appl. Surf. Sci. **148**, 223 (1999).
[30] J. H. Lee, J. H. Eun, S.Y. Park, S. G. Kim, and H. J. Kim, Thin Solid Films **435**, 95 (2003).
[31] B. Elidrissi, M. Addo, M. Regragui, C. Monty, A. Bougrine, and A. Kachouane, Thin Solid films **379**, 23 (2000).
[32] L. Rayleigh, Philos. Mag. **5**, 184 (1992).
[33] P. Scherrer, Göttinger Nachr. **2**, 98 (1918).
[34] M. Dhanam, R. Balasundar Prabhu, S. Jayakumar, P. Gopalakrishnan, and M. D. Kannan, phys. stat. sol. (a) **19**, 149 (2002).
[35] S. Velumani, Sa. Ka. Narayanadhas, and D. Mangalraj, Semicon. Sci. Tech. **13**, 1016 (1998).
[36] S. I. Jun, T. E. McKnight, M. L. Simpson, and P. D. Rack, Thin Solid Films **476**, 59 (2005).
[37] S. A. Chambers, Surf. Sci. Rep. **39**, 105 (2000).
[38] M. O. Aboelfotoh, K. C. Park, and W. A. Parkin, J. Appl. Phys. **48**, 2910 (1977).
[39] R. A. Nyquist and R. O Kagel, "Infrared Spectra of Complex Molecules", Academic, New York, (1971).
[40] H. Thomas, M. Epple, and A. Reller, Solid State Ionics **101-103**, 79 (1997).
[41] J. Gonioakowski and C. Noguera, Surf. Sci. **340**, 191 (1995).
[42] J. Gonioakowski and C. Noguera, Surf. Sci. **319**, 81 (1994).
[43] S. Russoy and C. Noguera, Surf. Sci. **262**, 259 (1992).
[44] E. Castanier and C. Noguera, Surf. Sci. **364**, 1 (1996).
[45] W. J. DeSisto and R. L. Henry, J. Cryst. Growth **101**, 314 (1991).

